SCI. MAR., 69 (2): 187-197 SCIENTIA MARINA 2005

Size structure of the planktonic community in microcosms with different levels of turbulence*

ANDRÉS CÓZAR [1,2] and FIDEL ECHEVARRÍA [1,3]

[1] Área de Ecología. Facultad de Ciencias del Mar y Ambientales. Universidad de Cádiz. 11510. Puerto Real. Cádiz. Spain.
[2] Present address: Dipartimento di Scienze Chimiche e dei Biosistemi, Università di Siena, Italy.
E-mail: cozar@unisi.it
[3] Centro Andaluz de Ciencia y Tecnología Marina. Universidad de Cádiz. 11510. Puerto Real. Cádiz. Spain.

SUMMARY: The evolution of a natural plankton community in two microcosms with well-differentiated turbulence levels (10^{-3} W m^{-3} and 10^{-1} W m^{-3}) was compared during artificially-generated blooms. Biomass-size spectra were used to assess the effects of the turbulent kinetic energy (TKE) on the plankton community. Picoplankton was the size range least affected. Indirect effects on picoplankton size structure were related to the TKE effects on the predators. Small nanoplankton represented a transitional size range in which small and variable TKE effects were observed. In the diatom size range, the positive TKE effect on these non-swimmers increased progressively with cell size. The results showed that TKE has a combined effect on both biomass and size structure because of the linkage between these community characteristics. On the whole, the changes observed in the community size structure would lead to the uptake of the maximum available free energy.

Keywords: turbulence, plankton size spectra, grazing resistant bacteria.

RESUMEN: ESTRUCTURA DE TAMAÑOS DE LA COMUNIDAD PLANCTÓNICA EN MICROCOSMOS CON DISTINTOS NIVELES DE TURBULENCIA. – En este trabajo se compara la evolución de una comunidad planctónica natural en dos microcosmos con distintos niveles de turbulencia (10^{-3} W m^{-3} y 10^{-1} W m^{-3}) durante una floración generada artificialmente. Se utilizó el enfoque basado en espectros de biomasa-tamaño con el fin de evaluar el efecto de la energía cinética turbulenta (ECT) sobre la comunidad planctónica. El picoplancton fue el rango de tamaños de la comunidad menos afectado, relacionándose los efectos indirectos observados en este rango con la influencia de ECT sobre sus depredadores. El nanoplancton pequeño representó un rango de transición en donde el efecto de ECT fue relativamente pequeño y variable. En el rango de tamaños de las diatomeas, el efecto positivo de ECT sobre la biomasa incrementó progresivamente con el tamaño de los organismos. Los resultados muestran un efecto combinado de la ECT sobre la biomasa total y sobre la estructura de tamaños de la comunidad, dos características de la comunidad que están relacionadas. En general, los cambios observados en la estructura de la comunidad permitirían la asimilación de la máxima energía libre disponible por parte de los organismos.

Palabras clave: turbulencia, espectros de tamaño del plancton, resistencia bacteriana a la depredación.

INTRODUCTION

There is increasing evidence that small-scale turbulence plays an important role in the plankton community (Marrasé *et al*., 1997 and references therein). Numerous examples can be found at both physiological and ecological levels. Physiological processes depend on the implications of the shear forces for the transport of molecules in and out of the organisms (e.g. Pahlow *et al*., 1997) and the structural vulnerability of cells and colonies (e.g. Berdalet and Estrada, 1993). The influence of small-scale turbulence on the behaviour of the organisms (e.g. Karp-Boss *et al*., 2000), encounter rates (e.g. Yamazaki *et*

*Received April 22, 2004. Accepted November 9, 2004.

al., 1991) and formation of microzones (e.g. Squires and Yamazaki, 1995) may also cause indirect effects on ecological interactions, especially predator-prey interactions (Peters *et al*., 2002).

Any flow of matter or energy through a pelagic ecosystem leaves its imprint on the structure of the plankton community (Rodríguez, 1994). Turbulent kinetic energy (TKE) represents a relevant input of auxiliary energy in the pelagic ecosystem. However, the diversity of processes directly or indirectly related to TKE hampers assessing the overall effect of this factor on the whole community. As there is a strong dependence of TKE effects on the body size of organisms (Lazier and Mann, 1989; Karp-Boss *et al*., 1996), we suggest the biomass-size spectrum as a tool for undertaking this task. Biomass-size spectra are the result of the combination of physiological (growth, respiration, etc.) and ecological (predation, competence, etc.) scales (Kerr and Dickie, 2001). Using recent approaches, the size spectra and derived parameters also allow the thermodynamic (Choi *et al*., 1999) and trophic (Kerr and Dickie, 2001; Cózar *et al*., 2003) analysis of the community. Linear size spectra result from a steady state in which predator-prey interactions generate a balanced flow of energy. From this state, fluctuations in energy inflow are accommodated by the size structure in order to accumulate the available free energy (e.g. TKE). The present work aims to characterise the turbulence effect along the plankton size spectrum using a comparative analysis of a natural community exposed to two different TKE levels.

MATERIAL AND METHODS

Artificial phytoplankton blooms were generated in two microcosms (area = 25×50 cm^2, depth = 30 cm) at two well-differentiated TKE levels: a low turbulence microcosm (LTM) and a high turbulence microcosm (HTM). Firstly, each enclosure was filled with 22.5 L of 0.7 μm-filtered seawater. This medium was enriched with nitrate (64 mmols), phosphate (9 mmols), silicate (2 mmols), micronutrients and vitamins (1-70 nmols). The N:P ratio of the addition was 7.3 (N-deficient). Then, each microcosm was completed with 2.5 L of natural seawater from the NW sector of the Alboran Sea, 30 miles offshore from Estepona. This area is characterised by frequent upwelling events.

Microcosms were kept at 18ºC and received a constant light intensity of 40 μE $m^{-2}s^{-1}$. Small-scale turbulence was generated through air bubbling. A fraction of the drag force of creeping flow around the bubbles is transformed into TKE. The turbulence dissipation rates were estimated according to Tatterson (1991). The air fluxes were 5 ml min^{-1} in LTM and 500 ml min^{-1} in HTM. Therefore, the turbulence dissipation rates were 10^{-3} W m^{-3} in LTM and 10^{-1} W m^{-3} in HTM. Both values correspond to TKE levels which would be relatively high in the ocean. The turbulence level applied in HTM could be considered an extreme level. It has been measured near the surface and in the zone of breaking waves (Johnson *et al*., 1994; Terray *et al*., 1996).

The development of the plankton blooms was monitored for 17 days. Water samples were collected every 2-3 days from an intermediate depth (15 cm from the bottom) and just on the bottom. Subsamples were used to estimate chlorophyll-*a* concentrations (*chl-a*) using a Turner Designs-10 fluorometer (calibrated with pure *chl a*, Sigma Co) following UNESCO (1994). Picoplankton sub-samples were fixed with glutaraldehyde (2% v/v) and nano- and microplankton sub-samples with lugol (1.5% v/v). Mesoplankton was absent during the experiment.

Two complementary microscopic techniques were employed to analyse the plankton samples (pico-, nano- and microplankton). Picoplankton was counted by epifluorescence microscopy (Leitz Laborloux microscope) with DAPI staining following Porter and Feig (1980). The organisms were measured at 1000x magnification using image analysis software (NIH *Image*). Biovolumes were calculated from geometric formulae with the best fit to cell shape. A morphological classification of the organisms was performed in this size range. Nano- and microplankton samples were processed with inverted microscopy at magnifications of 250x, 600x and 1000x (Uthermöhl, 1958). The organisms were measured with a semiautomatic image analysis system (Analytical Measuring Systems, VIDS V). Biovolumes were also calculated through geometric formulae. Taxonomic classifications were performed in these size ranges. The criterion adopted for scanning with both microscopic techniques was to measure more than 400 cells in each sample in order to keep the counting error within ±10% (Lund, 1945).

To build the biomass-size spectra, the organisms were arranged in size classes with increasing widths following a geometric 2^n series. With this partition, the amplitude of the size-class (Δw) coincides with

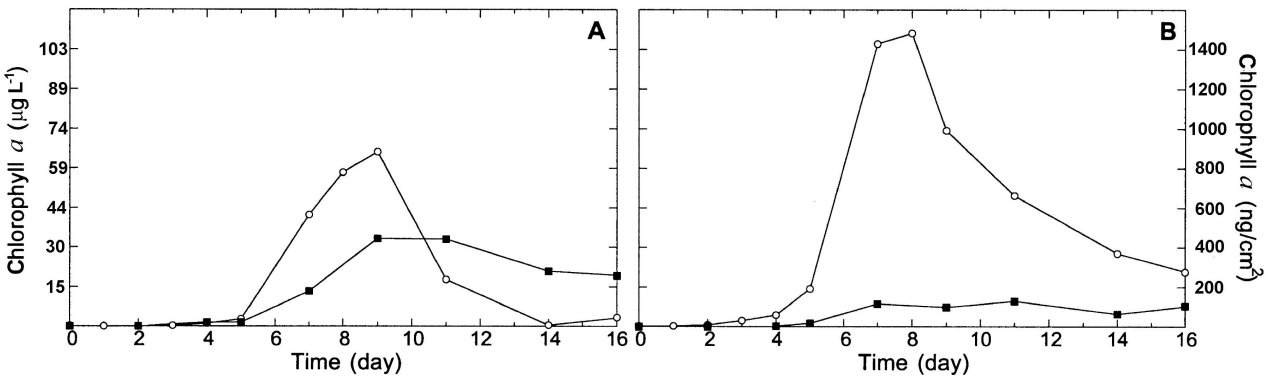

FIG. 1. – Temporal evolution of chlorophyll-*a* in the water column (white circles) and bottom (black square) during the experiment. Low turbulence microcosm (A) and high turbulence microcosm (B). Chlorophyll-*a* concentration is shown by volume (left scale) and area (right scale).

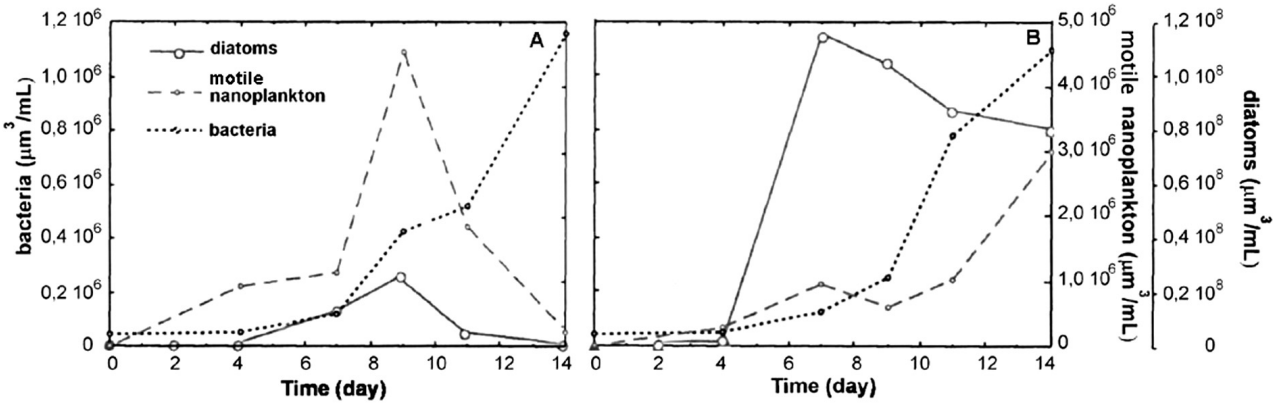

FIG. 2. – Temporal evolution of diatom biovolume, motile nanoplankton (flagellates and ciliates) and bacteria. Low turbulence microcosm (A) and high turbulence microcosm (B).

its lower limit (w). The normalised biomass in each class ($\beta(w_i)$) can be calculated from biomass (B) as:

$$\beta(w_i) = \frac{B(w, w + \Delta w)}{\Delta w} \ ,$$

When these data are plotted on a log-log axis, it is possible to obtain an overall parameterisation of the normalised biomass-size spectra (*NBSS*) as:

$$\log \beta(w) = a + s \log w$$

Comparative analyses of the plankton size structure in different systems are usually based on the parameters derived from the straight line fitted to *NBSS* (*e.g.* Kerr and Dickie, 2001; Rodríguez *et al.*, 2001). The intercept (a) expresses general abundance. The slope (s) gives a synthetic view of the relationship between the abundance of smaller organisms and larger ones. The correlation coefficient (R^2) of the regression can be used as a measurement of the total spectrum irregularity.

RESULTS

Dense blooms of phytoplankton were generated in both microcosms (Fig. 1). HTM showed higher total *chl-a* concentrations (mean 19 μg L^{-1}) than LTM (mean 15 μg L^{-1}). In the water column, the evolution of the blooms followed a classic pattern. Chlorophyll-*a* concentration increased exponentially, reaching 65 μg L^{-1} on Day 9 in LTM and 106 μg L^{-1} on Day 8 in HTM. Then, the blooms entered the senescent phase and *chl-a* decreased. The evolution of the *chl-a* in the bottom of LTM was coupled with the *chl-a* in the water column. In the bottom of HTM, the evolution of the *chl-a* was less variable.

Diatoms were the dominant planktonic group in both microcosms (Fig. 2). They were more abundant in HTM. Diatoms reached $2.4 \cdot 10^7$ µm^3 mL^{-1} on Day 9 in LTM and $11.0 \cdot 10^7$ µm^3 mL^{-1} on Day 7 in HTM. Motile plankton, however, showed a more favourable growth in LTM. Flagellates and ciliates reached 4.7 10^6 µm^3 mL^{-1} on Day 9 in LTM and 3.0 10^6 µm^3 mL^{-1} on Day 14 in HTM. Bacterial blooms

TABLE 1. – Characteristics of the main groups of plankton organisms identified in LTM (white strip) and HTM (grey strip). The percentage of biovolume in LTM is with respect to HTM.

	Size (μm^3)		Biovolume ($10^5 \mu m^3/mL$)			
	Mean	**S.D.**	**Maximum**	**Day**	**% in LTM**	
Rods & Cocci	0.09	0.07	1.6	14	52	
	0.07	0.06	1.3	14		
Bacteria aggregates	0.45	0.18	0.3	11	63	
	0.43	0.17	0.1	11		
Filaments	1.51	1.13	9.6	14	52	
	1.40	1.03	8.4	14		
Isochrysidales	8.6	6.1	9.0	4	46	
	8.5	6.6	7.5	7		
Chryptophycea	22	17	0.7	7	36	
	47	26	1.8	14		
Prymnesiales	52	35	3.2	9	100	
	-	-	-	-		
Prasinophyceae	60	34	10.9	9	64	
	89	71	9.8	14		
Dictyochophyceae	118	87	28.7	9	61	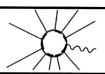
	124	70	17.9	14		
Cilliates	146	79	1.3 (1.0)	7 (14)	44	
	182	82	2.6	9		
Pseudonitzschia sp.	83	54	0.3	9	33	
	77	49	0.5	7		
Th. cf. allenii	307	222	48.9	9	96	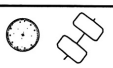
	595	254	1.4	9		
Chaetoceros spp.	537	413	0.9	9	2	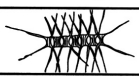
	5975	4705	68.4	9		
Skeletonema costatum	664	606	25.1	9	58	
	860	799	24.0	7		
Guinardia sp.	837	736	4.7	7	67	
	784	708	1.8	11		
Lauderia spp.	2459	496	0.8	11	1	
	23048	10806	62.0	11		
Th. cf. hyalina	6022	3541	159	9	8	
	6315	3729	1020	7		

in both treatments showed a similar evolution. Biomass increased exponentially when the phytoplankton concentrations decreased, reaching a maximum on Day 14 (1.16 10^6 μm^3 mL^{-1} in LTM and 1.10 10^6 μm^3 mL^{-1} in HTM).

A description of the main taxonomic and morphological groups classified in the enclosures is shown in Table 1. Diatoms were mainly represented by *Thalassiosira, Skeletonema, Chaetoceros* and *Lauderia*. *Thalassiosira spp*. was the dominant genus (> 70% of diatom biovolume in both microcosms). The dominant species were *T. cf. hyalina* and *T. cf. allenii*. A co-dominance of these two species was observed in LTM, while *T. cf. allenii* was practically absent in HTM. These species show well-differentiated body sizes. *T. cf. hyalina* had a mean cellular diameter of 26 μm (varying from 16 to 43 μm) while *T. cf. allenii* had a mean diameter of 11 μm (from 6 to 19 μm). A different species composition linked to different size distributions was also found within *Chaetoceros* and *Lauderia*. Nanoflagellates were classified at the level of taxonomic class. Prymnesiophyceae, Cryptophyceae, Prasinophyceae and Dictyochophyceae were present in the microcosms. The Prymnesiales and Isochrysidales orders (Prymnesiophyceae Class) were also differentiated due to their alternate occurrences and the evident morphological dissimilarities (with and without haptonema respectively). Ciliates were also found in both microcosms, although they only rep-

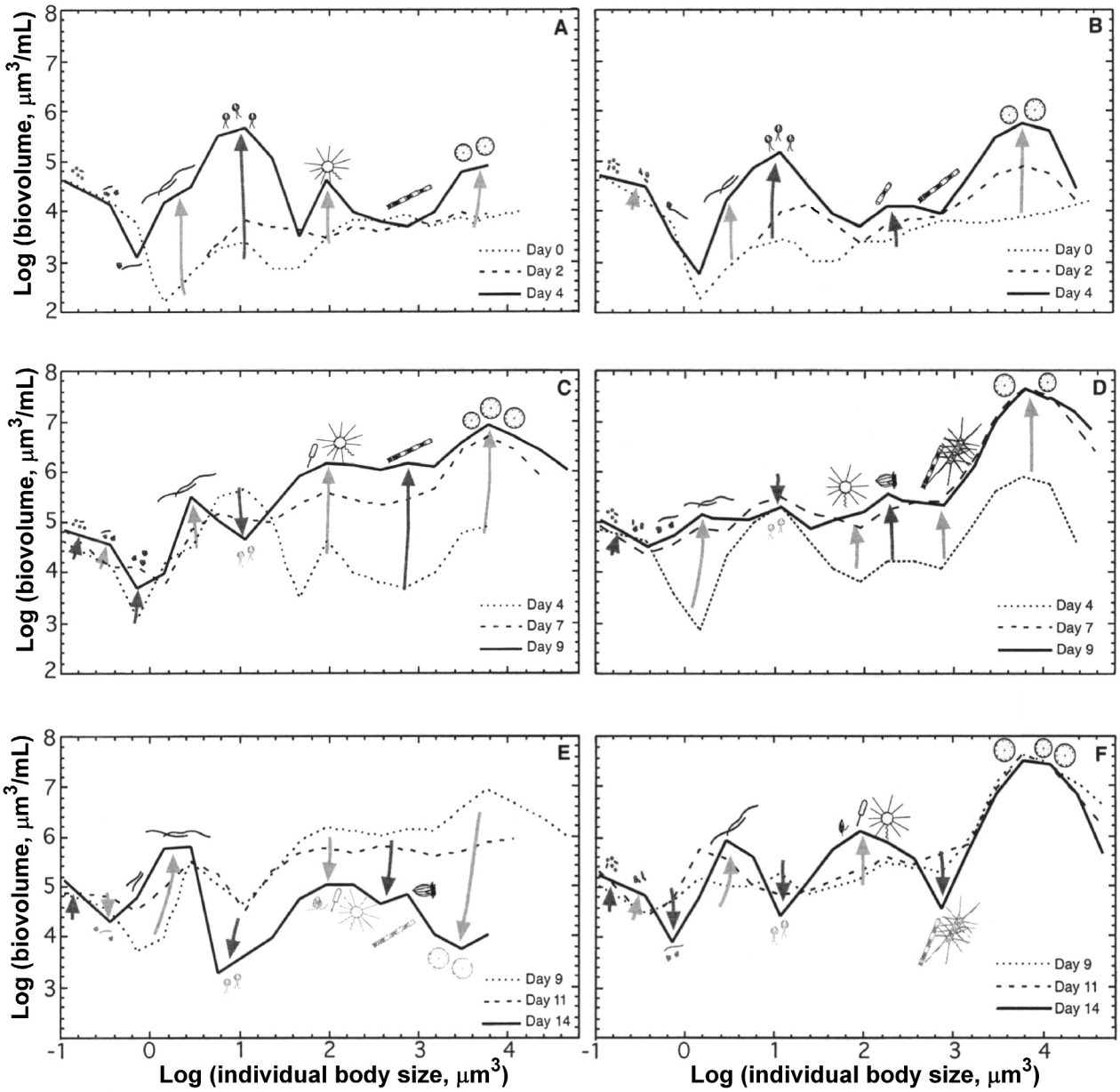

FIG. 3. – Temporal evolution of the biomass-size spectra in LTM (left column) and HTM (right column). Pre-bloom (A, B), bloom (C, D) and post-bloom phases (E, F). The main organisms causing biomass irregularities along the size spectra are illustrated (see Table 1).

TABLE 2. – Sherwood numbers estimated for the swimming activity, the sedimentation process and the compared TKE levels in organisms of 1 and 10 μm of equivalent spherical diameter (ESD). Estimates were made following Kiṣrboe (1993).

ESD (μm)	Swimming speed (μm s^{-1})	Sedimentation speed (μm s^{-1})	Sherwood numbers due to Swimming	Sedimentation	TKE in LTM	TKE in HTM
1	93	0.03	1.23	1.00	1.00	1.02
10	160	2.73	5.26	1.11	1.06	1.21

resented 5.1% of the total biovolume of motile plankton. The different groups of motile organisms showed a temporal coupling, appearing as a succession of biomass peaks: small phytoflagellates, ciliates, large flagellates and a second peak of ciliates (Table 2). Small phytoflagellates were composed of Isochrysidales. Large flagellates showed higher abundance and trophic diversity. They were mainly composed of Dictyochophyceae and Prasinophyceae. The succession described was observed in

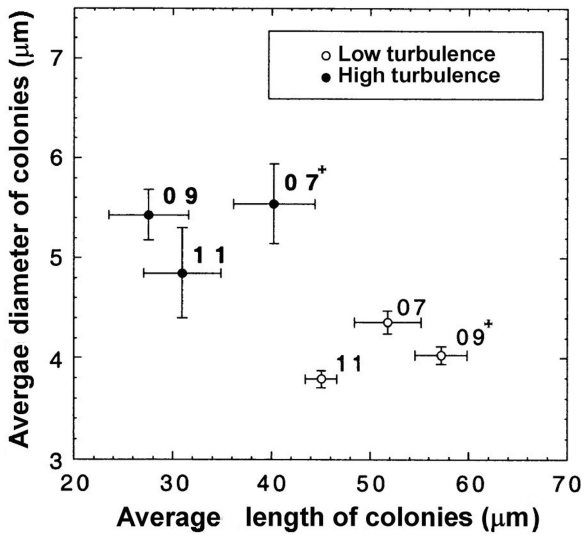

FIG. 4. – Length and width of *Skeletonema costatum* colonies during the bloom phase (Days 7, 9 and 11). Stars indicate the day of the biomass peak. Crossed bars show the standard errors.

both microcosms, although it was delayed 2-3 days in HTM. Bacterioplankton was composed of filamentous bacteria, free bacteria (rods and cocci) and bacterial aggregates. Filamentous bacteria were the dominant morphotype (> 85% of bacterial biovolume in both microcosms). Some cyanobacteria were also observed during the last days of the experiment.

A general view of the plankton dynamics is shown in Figure 3. On Day 2, small flagellates (Isochrysidales) began to grow in both treatments (Fig. 3A and 3B). On Day 4, small flagellates reached their maximum biovolume in LTM and large flagellates also began to grow in this microcosm. During the bloom phase (Fig. 3C and 3D), LTM contained a rich community of large flagellates (Dictochophyceae, Prasinophyceae) and small flagellates were practically absent. In HTM, this shift ended during the post-bloom. In both microcosms, *Thalassiosira spp*. reached their maximum mean cell size during the biomass peak. During the post-bloom (Fig. 3E and 3F), cells rapidly disappeared from the water column in LTM. In HTM, *T. hyalina* maintained a relatively high biomass until the end of the experiment.

The diameters of the dominant diatom species (*Thalassiosira cf. hyalina*, *Skeletonema costatum*) were significantly ($P < 0.001$) greater in HTM (Fig. 4). The length of the diatoms may increase greatly due to colony formation. However, colony-forming diatoms appeared mainly as single cells, especially *Thalassiosira spp*. The 23% (in biovolume) of *Thalassiosira spp*. was grouped in colonies in LTM and 1% in HTM. *Thalassiosira* formed few colonies, probably as a result of the relative fragility of the colonies. The longest colonies were formed by *S. costatum*. These colonies also reached the largest size during the biomass maximum and were significantly ($P < 0.001$) longer in LTM (Fig. 4). Diatom colonies seemed to be highly vulnerable to the levels of TKE studied. In the picoplankton, we did not found significant differences between the morphological characteristics (length and width) of rods and cocci or bacteria aggregates. Likewise, differences between the averaged lengths of filamentous bacteria or cyanobacteria were not observed.

The parameters derived from the NBSS linearisation were used to compare the community size structures (Fig. 5). The regression coefficient (R^2) was generally higher in LTM, indicating higher spectra regularity. Steeper slopes (s) were found in LTM, indicating dominance by small organisms. Temporally, slopes decreased during the bloom phase. A compilation of slopes of plankton size

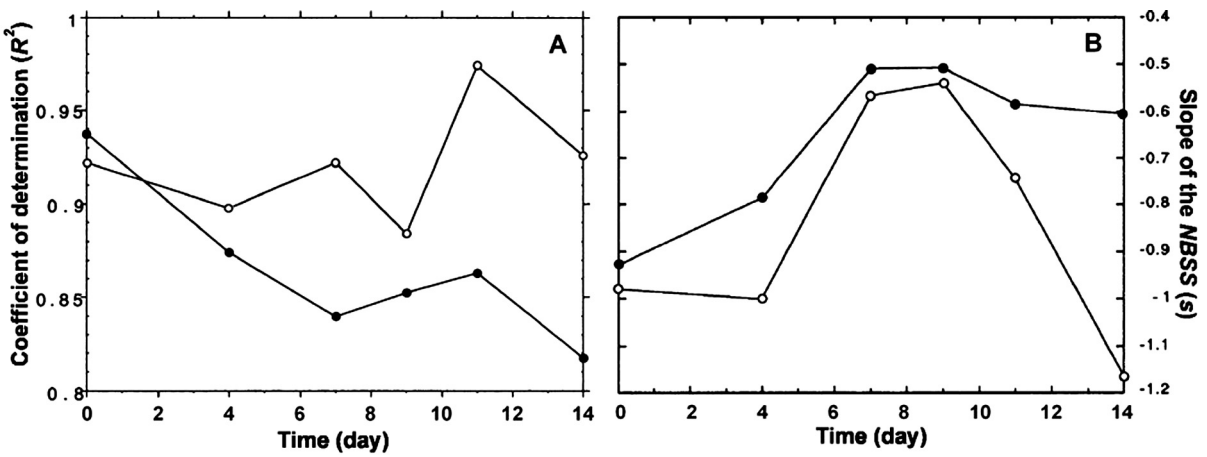

FIG. 5. – Temporal evolution of the lineal regression coefficient (R^2, B) and the slope (s, A) of the normalised biomass-size spectra. LTM (white points) and HTM (black points).

spectra in natural systems shows a range of variation from -1.34 to -0.62 (Choi *et al.*, 1999). During the bloom phase, we observed extremely low slopes, especially in HTM (s = -0.51). These values could be related to the unusually high TKE and *chl-a* concentrations in the enclosures.

DISCUSSION

The different timing and magnitude of the phytoplankton response suggested a generally positive effect of the TKE on the growth of the organisms (Fig. 1). The higher spectra irregularity of HTM (lower R^2, Fig. 5A) can be interpreted as a stronger disturbance of the steady state resulting from higher inflow of matter in the community (e.g. Cózar *et al.*, 2003). Both microcosms were equally enriched, but TKE seems to affect the matter flux transferred to the plankton community. Small-scale turbulence, such as swimming or sedimentation, diminishes the microzone of laminar shear (diffusive boundary layer) surrounding the cells, facilitating physical-chemical interchange with the fluid by advection. It is known from previous studies that the advection effect is stronger in larger organisms (Lazier and Mann, 1989; Karp-Boss *et al.*, 1996). This study shows the predominance of large-sized organisms in a plankton community exposed to higher levels of TKE (less negative s, Fig. 5B). In LTM, small-sized organisms may benefit from the smaller surface to volume ratio (S/V), which favours nutrient uptake (Munk and Riley, 1952).

Thalassiosira cf. hyaline was the major species involved in changes in the community structure, composing the highest biomass accumulation along the spectra (Fig. 3). This species had the largest cell size of those in the microcosms. Only some colonies of *Lauderia sp*. in HTM were larger (Table 1). The potential diffusive nutrient supply is greater for solitary cells than for chains of similar volume or similar advective supply (Pahlow *et al.*, 1997). The ability of diatoms to form colonies may result in an overall increase in the size of the organisms. Nevertheless, only chains with large spaces between cells (e.g. *Skeletonema sp*., *Thalassiosira sp*.) can overcome this disadvantage, and may even obtain a higher nutrient supply than do solitary cells (Pahlow *et al.*, 1997). However, the levels of TKE studied were enough to break this type of colonies (Fig. 4), and the large cells of *T. cf. hyaline* were the dominant morphotype. Schöne (1970) also reported the possibility of colony breaking for species such as *Skeletonema costatum*.

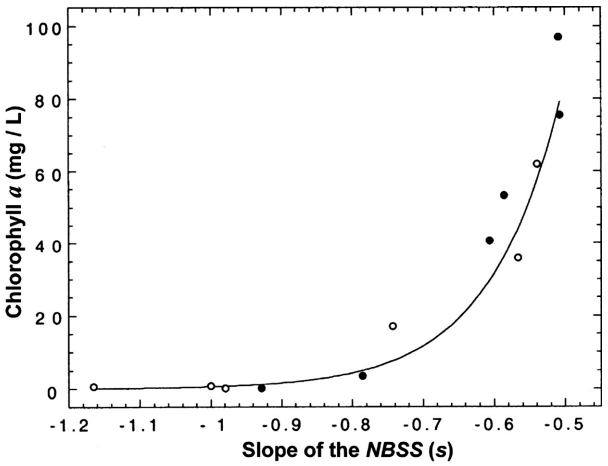

FIG. 6. – Slope of normalised biomass-size spectra against chlorophyll concentration. LTM (white points) and HTM (black points).

The influence of algal biomass on the observed changes in the plankton structure was considerable. Chlorophyll-*a* explained 94% of the variability of spectrum slope (Fig. 6). The use of the slope represents a consistent parameterisation of the size structure of the whole community. Classical studies have conceptually related body size and biomass (Margalef, 1978). Small plankton characterises stagnant and oligotrophic waters, while larger cells dominate eutrophic and turbulent waters. The succession between large diatoms and nanoflagellates often occurs during the seasonal cycle (Kiørboe, 1993). Figure 6 shows the linkage between biomass and size structure over a shorter timescale. This linkage was common for both treatments. Thus, TKE had a combined effect on both biomass and size structure following a common pattern. This pattern was exponential and showed higher abundance of large-sized organisms with increasing biomass in the community. The rapid change in the size structure when s values are in the interval (-1.2, -0.7) may be a result of the adaptability of the community to using the free energy (nutrients and TKE) available in the enclosures. Thermodynamically, the principle of least specific dissipation indicates that any system will tend towards a local minimum in the rate of energy dissipation per unit biomass so as to accumulate the maximum energy (Prigogine, 1955). Choi *et al.* (1999) showed that the possibility of modifying the energy dissipation rate in nature is restricted to the interval (-1.2, -0.7). Less negative slopes (abundant large-sized organisms) are related to communities with a lower energy dissipation rate, which reaches the min-

imum value when s = -0.7. In this study, we observed a positive correlation between biomass and size but high increases in biomass did not significantly modify the size structure beyond *s* = -0.7. On the other hand, rapid changes in community structure associated with fluctuations in energy influxes are thermodynamically unsteady and the energy excesses (located in biomass accumulations along the spectra) are rapidly relaxed (Kerr and Dickie, 2001; Cózar *et al.*, 2003). Slopes of both microcosms suddenly decreased when the availability of free energy diminished in the post-bloom (Fig. 5B).

Intra-specific variability in the body size of the main species contributed to maintaining the biomass-size linkage in the community (Fig. 4). At short time scales, the ontogenic adjustments of the population are particularly significant (Jiménez *et al.*, 1987). Nevertheless, differences in taxonomic composition are also necessary to increase the variability of the size structure. The most relevant example was the absence of *T. cf. allenii* in HTM. The average cellular diameter of this species was 58% smaller than *T. cf. hyalina*. The development of swimming capacity was also different and cellular motility was a more common strategy in LTM. Likewise, flagellates and ciliates grew rapidly in this enclosure.

Evidence of the influence of TKE on bacterial uptake remains less clear (Logan and Kirchman, 1991). Differences between the averaged lengths of filamentous bacteria were not found with the TKE levels compared. Nevertheless, the maximum size of filamentous bacteria was different in the two enclosures. Indirect effects of turbulence on bacterial abundance have been related to the influence of TKE on the coupled food web (Peters *et al.*, 2002). In each microcosm, the maximum bacterial size coincided with the respective biomass peaks of proto-zooplankton (flagellates and ciliates). Concepts such as size thresholds for predation are essential for explaining these results (Jürgens *et al.*, 1999; Prieto *et al.*, 2002). There is a size range affected by predation, the smaller and larger cell sizes appearing to be a refuge. Alterations of the prey size distribution may be expected as result of trophic relations (Benoit and Rochet, 2004). We found a significant correlation between the average size of potential prey and the biomass of the potential predators (Fig. 7). A common pattern of predator-prey interaction was observed for both microcosms. However, the different temporal evolution of the predators resulted in small temporary differences in the bacteria size distribution.

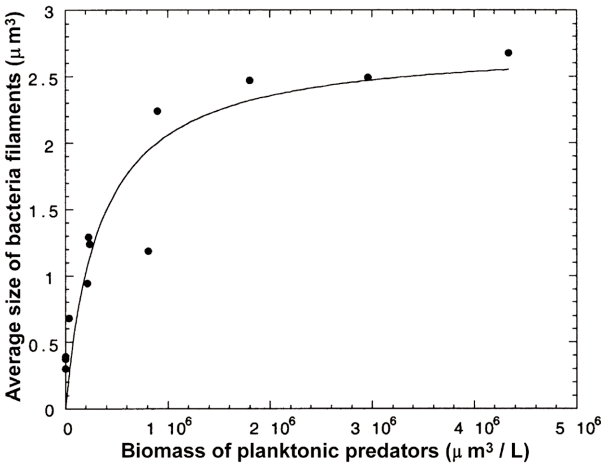

FIG. 7. – Average size of bacteria filaments versus flagellate biovolume. The regression line (R = 0.923, P < 0.001) follows the Michaelis-Menten equation: S = (Smax B) / (K + B), where S is the bacterial size (mm^3) and B is the biomass of potential prey (mm^3 / L). The growth of the filamentous bacteria showed a maximum threshold (Smax) of 2.75 mm^3.

Assessing the influence of turbulence along the planktonic size spectra

By comparing the size spectra of both microcosms, an assessment of the TKE effects along the plankton size spectrum can be made. The similarity or divergence of the spectra would indicate a lower or higher influence of TKE on the different size classes. Due to the wide range of biomass values along the spectrum, we quantified the differences of biomass in each size class through a logarithmic subtraction: log $(B(w_i)_{LTM} / B(w_i)_{HTM})$. Three planktonic size intervals were identified: picoplankton, small nanoplankton and diatoms (Fig. 8).

Picoplankton was mainly represented by the bacterioplankton. In the ocean, picoplankton abundance tends to be constant regardless of the temperature, salinity or nutrient concentrations (Fogg, 1986). Figure 8 also seems to support constancy in relation to TKE. This interval showed the smallest differences between the spectra of LTM and HTM.

Small nanoplankton was mainly composed of flagellates. The slight difference in the spectra of the two treatments does not show a clear relation of the biomass to the TKE level or body size. The influence of TKE on the transport of substances in and out of the motile organisms seems to be highly variable. Flagellates and ciliates often use swimming or self-generated currents to increase the encounter rate with prey. The prey perception may be harmed in most flagellates, especially among predators perceiving the prey in a chemical or mechanical way (Kiørboe, 1997). However, helioflagellates such as

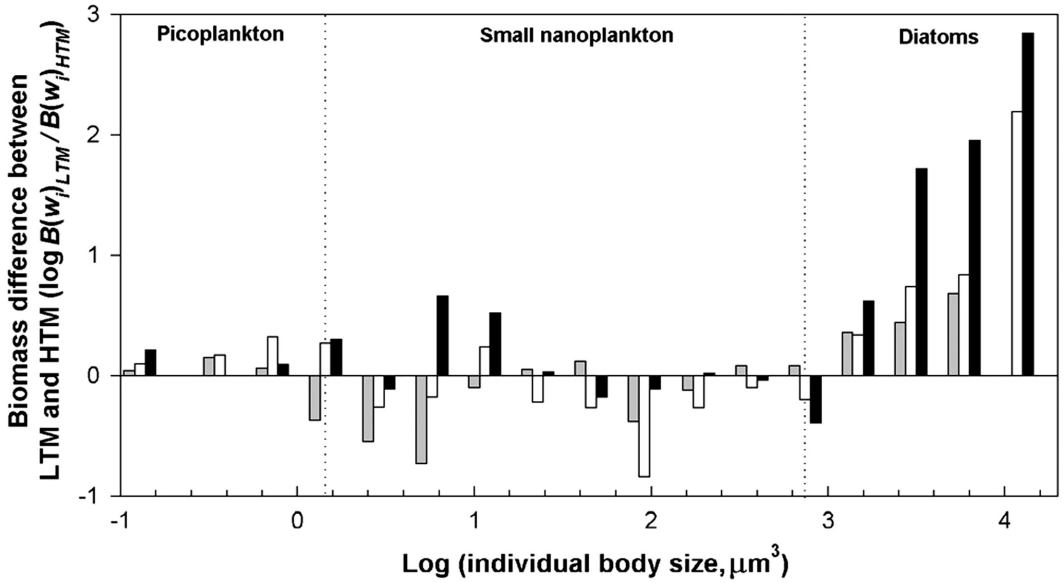

FIG. 8. – Biomass differences between the spectra of LTM and HTM during the phases of pre-bloom (grey bars), bloom (white bars) and post-bloom (black bars). Positive values indicate higher biomass in HTM. Three size ranges have been differentiated: picoplankton, small nanoplankton and diatoms intervals. The limits between intervals are indicated with dotted lines and correspond approximately to 1 and 10 μm ESD.

Dyctochophyceae (the dominant motile group) are stationary when feeding. These organisms depend on the prey motility and small-scale turbulence to find prey (Shimeta and Jumars, 1991). The prey are caught when they touch a sticky pseudopod. Other examples even show a reduction in the assimilation of inorganic nutrients as a result of TKE effects (Karp-Boss *et al*., 1996). This complexity, together with the diversity of flagellates composing the nanoplankton range, could explain the variable influence of TKE on this size interval.

The diatom interval showed the clearest differences between the two microcosms. Arin *et al*. (2002) showed that the relative contribution of diatoms to phytoplankton biomass increases in turbulent environments. We found a divergence of the spectra as size increased in the diatom interval. The highest difference between the two spectra (or the highest influence of TKE) was observed during the post-bloom. This result is probably related to the importance of nutrient availability on the magnitude of the TKE effects (Arin *et al*., 2002). Advective or diffusive transport supplies nutrients in the vicinity of the cell. However, when the environmental nutrient concentrations are high, phytoplankton cannot completely absorb all the nutrients that diffusion and advection are able to supply. During the post-bloom, when nutrients are exhausted, the possible advantages of turbulent advection would be more significant.

The combined effects of small-scale turbulence and sedimentation would explain the divergence of the spectra of the two microcosms along the diatom size interval. The influence of small-scale turbulence in reducing the diffusive boundary layer around the organisms increases with body size (Lazier and Mann, 1989; Karp-Boss *et al*., 1996). On the other hand, a different plankton vertical distribution occurred in the two enclosures as a result of the large-scale turbulence. The mean proportion of *chl-a* in the bottom to total *chl-a* was 0.13 in HTM and 0.50 in LTM. The higher resuspension of large organisms in HTM involved large organisms in a rapid resuspension-sedimentation cycle. In the open ocean, similar mechanisms re-introduce large organisms into the euphotic zone (Rodríguez *et al*., 2001). The effect of sedimentation on the diffusive boundary layer is also positively related with size through Stokes's law.

The Sherwood number (*Sh*) is the dimensionless relation between the rate of mass transport by advection and by diffusion in the cell (see Kişrboe, 1993). If the advective transport is zero, *Sh* is 1. This parameter allows the theoretical size-based assessment of the different effects of sedimentation, swimming and TKE on the uptake kinetics (Table 2). Sedimentation and TKE have significant effects on the organisms larger than 10 μm because of the dramatic decrease in the diffusive transport with body size. The uptake by diffusion is inversely related to the square of size. Thus, an increase from 1 to 10 μm would cause a 100-fold decrease in the diffusive transport. The effect of the swimming

capacity on nutrient uptake was, however, significant in small-sized organisms. The advantages of the swimmer capacity increase considerably with body size. The advantages offered by both sedimentation and TKE (Sh = 1.11 and Sh = 1.21 respectively) would not explain the absence of motile organisms larger than 10 μm. The effect of swimming would be more favourable (Sh = 5.26). However, the survival strategy of the motile organisms shows a higher dependence on their motility and structural integrity. The behavioural changes or cellular damage caused by TKE (e.g. Berdalet and Estrada, 1993; Karp-Boss *et al*., 2000) could hamper the occurrence of large-sized swimmers. In the microcosms, the effect of the shear forces on the larger organisms has been demonstrated with the colonies breaking. Indeed, only small nanoplankton was able to use a strategy of "swimming" instead of "sedimentation and turbulence".

The present study shows a progressive increase in TKE effects towards large non- motile organisms. Biomass-size spectra started diverging above 10 μm of ESD. This result agrees with the estimations of Lazier and Mann (1989). Using a one-order lower shear rate, these authors established 100 μm as the threshold at which TKE starts having significant effects. The physical dependence of the diffusive and advective transport on body size and the detrimental effects of TKE on large motile organisms suggest the existence of a typical pattern of TKE influence along the plankton size spectra. Nevertheless, future studies are necessary to test how repeatable these findings are.

ACKNOWLEDGEMENTS

The present study was conducted under a Spanish National Plan of Marine Science and Technology sponsored research programme (MAR96-1837). We thank Roger Harris (Plymouth Marine Laboratory, UK) and anonymous reviewers for comments and suggestions on an earlier version of the manuscript.

REFERENCES

Arin, L., C. Marrasé, M. Maar, F. Peters, M.M. Sala and M. Alcaraz. – 2002. Combined effects of nutrients and small-scale turbulence in a microcosm experiment. I. Dynamics and size distribution of osmotrophic plankton. *Aquat. Microb. Ecol.*, 29: 51-61.

Benoit, E. and M.J. Rochet. – 2004. A continuous model of biomass size spectra governed by predation and effects of fishing on them. *J. Theor. Biol.*, 226: 9-21.

Berdalet E. and M. Estrada. – 1993. Effects of turbulence on several dinoflagellate species. In: T.J. Smayda and Y. Shimizu (eds.). *Toxic Phytoplankton Blooms in the Sea*, pp. 773-740. Elsevier, New York.

Choi, J.S., A. Mazumder and R.I.C Hansell. – 1999. Measuring perturbation in a complicated, thermodynamic world. *Ecol. Model.,* 117: 143-158.

Cózar, A., C.M. García and J.A. Gálvez. – 2003. Analysis of plankton size spectra irregularities in two subtropical shallow lakes (Esteros del Iberá, Argentina). *Can. J. Fish. Aquat. Sci.*, 60: 411-420.

Estrada, M., and E. Berdalet. – 1997. Phytoplankton in a turbulent world. In: C. Marrasé, E. Saiz and J.M. Redondo (eds.). *Lectures on plankton and turbulence. Sci. Mar.*, 61(Suppl.1): 125-140.

Fogg, G.E. – 1986. Picoplankton. *Proceedings of the Royal Society of London,* 228: 1-30.

Jiménez, F., J. Rodríguez, B. Bautista and V. Rodríguez. – 1987. Relations between chlorophyll, phytoplankton cell abundance and biovolume during a winter bloom in Mediterranean coastal waters. *J. Exp. Mar. Biol. Ecol.*, 105: 161-173.

Johnson, G.C., R.G. Lueck and T.B. Sandford. – 1994. Stress on the Mediterranean outflow plume: Part II. Turbulent dissipation and shear measurements. *J. Phys. Oceanogr.,* 24: 2084-2092.

Jürgens, K., J. Pernthaler, S. Schalla and R. Amann. – 1999. Morphological and compositional changes in a planktonic bacterial community in response to enhanced protozoan grazing. *Appl Environ. Microbiol.,* 65: 1241-1250.

Karp-Boss, L., E. Boss and P.A. Jumars. – 1996. Nutrient fluxes to planktonic osmotrophs in the presence of fluid motion. *Oceanogr. Mar. Biol. Ann. Rev.,* 34: 71-107.

Karp-Boss, L., E. Boss and P.A. Jumars. – 2000. Motion of dinoflagellates in a simple shear flow. *Limnol. Oceanogr.*, 45(7): 1594-1602.

Kerr, S.R., and L.M. Dickie. – 2001. *The biomass spectrum; a predator-prey theory of aquatic production*. Columbia University Press, New York.

Kiørboe, T. – 1993. Turbulence, phytoplankton cell size and the structure of pelagic food webs. In: J.H.S. Blaxter and A.J. Southward (eds.). *Advances in Marine Biology*, 29: 1-72. Academic Press Ltd., San Diego.

Kiørboe, T. – 1997. Small-scale turbulence, marine snow formation, and planktivorous feeding. In: C. Marrasé, E. Saiz and J.M. Redondo (eds.). *Lectures on plankton and turbulence. Sci. Mar.*, 61(Suppl.1): 141-158.

Lazier, J.R.N. and K.H. Mann. – 1989. Turbulence and diffusive layers around small organisms. *Deep-Sea Res. A*, 36: 1721-1733.

Logan, B.E. and D.L. Kirchman. – 1991. Uptake of dissolved organics by marine bacteria as function of fluid motion. *Mar. Biol.*, 111: 175-181.

Lund, J.W.G. – 1945. Observations on soil algae, I: The ecology, size and taxonomy of British soil diatoms. *New Phycol.,* 44: 196-219.

Margalef, R. – 1978. Life-forms of phytoplankton as survival alternatives in an unstable environment. *Oceanol. Acta,* 1: 493-509.

Marrasé C., E. Saiz and J. Redondo (eds.). – 1997. *Lectures on Plankton and Turbulence. Sci. Mar.,* 61 (Suppl.1).

Munk, W.H. and G.A. Riley. – 1952. Absorption of nutrients by aquatic plants. *J. Mar. Res.*, 11: 215-240.

Pahlow, M., U. Riedesell and D.A. Wolf-Gladrow. – 1997. Impact of cell shape and chain formation on nutrient acquisition by marine diatoms. *Limnol. Oceanogr.,* 42(8): 1660-1672.

Peters F., C. Marrasé, H. Havskum, F. Rassoulzadegan, J. Dolan, M. Alcaraz and J.M. Gasol. – 2002. Turbulence and the microbial food web: effects on bacterial losses to predation and on community structure. *J. Plankton Res.*, 24: 321-331.

Porter, K.G. and Y.S. Feig. – 1980. The use of DAPI for identifying and counting aquatic microflora. *Limnol. Oceanogr.*, 25: 943-948.

Prieto, L., J. Ruiz, F. Echevarría, C.M. García, A. Bartual, J.A. Gálvez, A. Corzo and D. Macías. – 2002. Scales and processes in the aggregation of diatom blooms: high time resolution and wide size range records in a mesocosm study. *Deep Sea Res.*, 49: 1233-1253.

Prigogine, I. – 1955. *Thermodynamics of Irreversible Processes*. John Wiley and Sons, New York.

Rodríguez, J. – 1994. Some comments on the size-based structural analysis of the pelagic ecosystem. In: J. Rodríguez and W.K.W. Li (eds.). *The size structure and metabolism of the pelagic ecosystem. Sci. Mar.,* 58 (Supl. 1-2): 1-10.
Rodríguez, J, J. Tintoré, J.T. Allen, J.M. Blanco, D. Gomis, A.Reul, J. Ruiz, V. Rodríguez, F. Echevarría and F. Jimenez-Gómez. – 2001. Mesoscale vertical motion and the sizestructure of phytoplankton in the ocean. *Nature,* 410: 360-363.
Schöne, H. – 1970. Untersuchungen zue okologischen Bedeutung des Seegangs fur das Plakton mit besonderer Berucksichtigung mariner Kieselalgen. *Int. Rev. Ges. Hydrob.,* 55: 595-677.
Shimeta, J. and P.A. Jumars. – 1991. Physical mechanisms and rates of particle capture by suspension feeders. *Oceanogr. Mar. Biol. Annu. Rev.*, 29: 191-257.
Squires, K. and H. Yamazaki. – 1995. Preferential concentration of marine particles in isotropic turbulence. *Deep Sea Res.*, 42: 1989-2004.
Tatterson, G.B. – 1991. Fluid mixing and gas dispersion in agitated tanks. *McGraw-Hill, Inc.*, New York.
Terray, E.A., M.A. Donelan, Y.C. Agrawal, W.M. Drennan, K.K. Kahma, A.J. Williams, P.A. Hwang and S.A. Kitaigorodskii. – 1996. Estimates of kinetic energy dissipation under breaking waves. *J. Phys. Oceanogr.*, 26: 792-807.
UNESCO. – 1994. Protocols for the Joint Global Ocean Flux Study (JGOFS) Core Measurements, Manual and Guides 29, 170pp.
Utermöhl, H. – 1958. Zur vervollkommnung der quantitativen phytoplankton-methodik. *Mitt. int. Ver. Theor. augem. limnol.* 9: 1-38.
Yamazaki, H., T.R. Osborn and K.D. Squires. – 1991. Direct numerical simulation of planktonic contact in turbulent flow. *J. Plankton Res.*, 13: 629-643.

Scient. ed.: T. Kiørboe